Motion sensing study on a mobile robot through simulation model and experimental tests

PIERANGELO MALFI, ARMANDO NICOLELLA, MARIO SPIRTO, CHIARA COSENZA,
VINCENZO NIOLA*, SERGIO SAVINO
Department of Industrial Engineering
University of Naples Federico II
Via Claudio 21 – 80125, Naples, Italy
ITALY

Abstract: - The employment of mobile robots, remotely or autonomously controlled for field operations, is an emerging topic. The development of suitable simulation models can aid the design and testing of such mobile robots. Here a small commercial prototype of a Rocker-Bogie Rover has been employed in experimental tests compared to simulations on a multibody model. In particular, the tests have dealt with the acquisition and processing of accelerometer signals both on experimental prototype and in simulation environment. The paper proposes a real time signal processing approach that could aid the motion planning and rover navigation control.

Key-Words: - Rover, Rocker-Bogie, signal processing, FFT, IMU

Received: May 15, 2021. Revised: April 17, 2022. Accepted: May 16, 2022. Published: July 6, 2022.

1 Introduction

In last years, academic community and industry have been showing a growth of interest in unmanned service robotics and vehicles for field operations [1],[2],[3],[4]. For instance, some autonomous vehicles have been designed for agricultural tasks [5],[6],[7]. Field operation rovers, similarly, to space exploration rovers such as Curiosity and Perseverance, are autonomous or remotely controlled vehicles able to tread on uneven terrain [8] and perform several operations [9],[10].
The object of this paper is a small rover prototype that is equipped with a suspension system named Rocker-Bogie [11], employed in some of most recent Mars exploration rovers.
The Rocker-Bogie [12],[13],[14],[15] is an articulated, passive suspension system whose purpose is to provide stability to a six-wheeled rover over rough terrain in a slow speed mode. The adoption of this articulated suspension system allows all wheels to keep contact on the ground and be independently actuated by six motors. The geometry of the suspension is designed so that the weight of the vehicle can be assumed equally distributed among the wheels of the rover. A schematic representation of this suspension system is shown in Fig. 1.

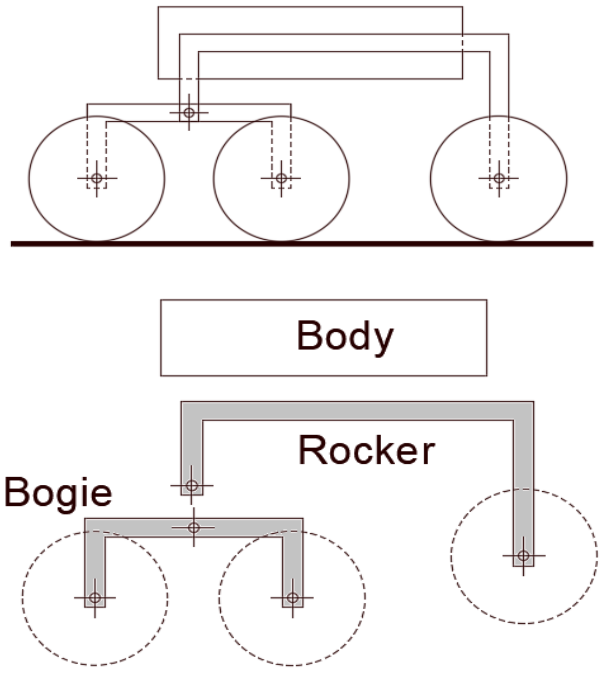

Figure 1 –Rocker-Bogie suspension system: sketch and schematic representation of the main parts.

One of the main challenges with this type of system is the control of the trajectory followed by the rover. To face this problem, the employment of vision

system can enhance robot trajectory control [16], [17]. C. Chen et al. [18] developed a method to control a planetary rover trajectory based on both kinematic and dynamic control, using rover motion data and the forces acting on it. The acquired data from such controls are angular velocities which, appropriately processed by the controller, serve as inputs to the motors. Such control system makes possible to decrease the internal forces acting between the same side wheels at least 60 percent and, at the same time, obtain the pursuit of the desired trajectory.
S. Wu et al. [19] developed a control algorithm, based on exponential type law, on the traction coordination of a lunar rover traveling over rough terrain. The algorithm is designed to optimize the traction force and minimize the slip ratio, control the velocity and normal force. The validity of the proposed algorithm has been demonstrated through simulations for a rover moving along slopes and ditches. The proposed approach can minimize slip ratios and mechanical wear and tear, improve mobility, and increase the overall durability of the rover. The enrichment of multibody simulation model with experimental data such as vision data has been showed in previous works in robotics context [20],[21],[22]. M. Thianwiboon et al [23], starting from the study of the kinematics of a six-wheeled rover with Rocker-Bogie suspension, developed a traction control system (TCS) based on the slip angle that is estimated from the experimental measurement of the rolling speed of the wheels and the rover velocity, through both simulation and experimental tests. In a previous work [24], the study of the variation in the distribution of the load among the wheels has been presented for a rover. In addition, the rover stability has been studied for different ground geometries through a kinematic analysis to define the suspension configuration as a function of ground geometry. Moreover, it has been evaluated the possibility of equipping the passive hinge, that connects the rocker with the bogie, by a torsional adjustable preloaded spring [25].
In this paper, a signal processing approach has been proposed through the introduction of a new parameter that can be used as an additional index for motion planning of a six-wheeled rover featured by Rocker-Bogie suspension system. The adoption sophisticated signal processing has allowed easier control of complex systems [26].

2 Prototype and Multibody Model

A prototype rover with Rocker-Bogie suspension (mentioned above) was built to make a comparison between experimental analysis and computer simulation results. Several software have been employed to create a multibody model for the simulations. The Rover prototype is presented in Fig. 2.

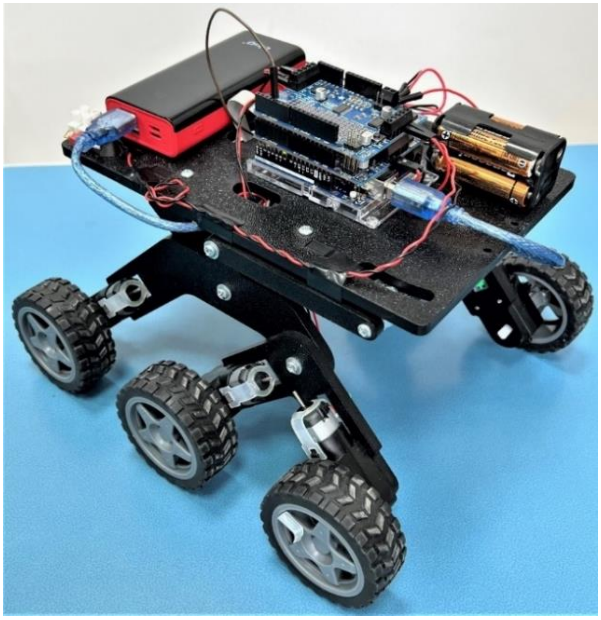

Figure 2 – Rover prototype.

The prototype (manufactured by Actobotics®) is composed by: articulated chassis, six wheels, and six motors. Simplicity, low cost, and low weight led to this choice. The chassis is ABS 3D printed and is sized in order to have similar vertical loads on the six wheels while their axes are on the same horizontal plane. The six non-steered wheels rover changes trajectory by skid steering [27]. On the tire tread there are four lines of twenty-four tire blocks circumferentially organized. Each DC electric motors (TT Right Angle Gear Motor type) is coupled to a gearbox (48:1 gear ratio) that slows down the rotation and changes the direction of output shaft.
The hardware for rover control consists of an Arduino Uno WiFi Rev 2 controller board and two Adafruit Motor Shield V2 boards for the six motors drive. To avoid voltage drops, two different power systems were used: a battery pack consisting of 4 AA batteries (1.5 V each) used to power the controller, and a 5 V, 2A USB powerbank to power the motor shields. A communication logic based on the User Datagram Protocol (UDP) was used for WiFi remote control. For this purpose, the Osoyoo WiFi UDP Robot Car Controller App was chosen: this App is preset to control a mobile robot by sending commands by sending alphanumeric characters. The CAD was modelled in Solidworks®, which was then imported into the MatLab®/Simulink® environment for multibody modeling.

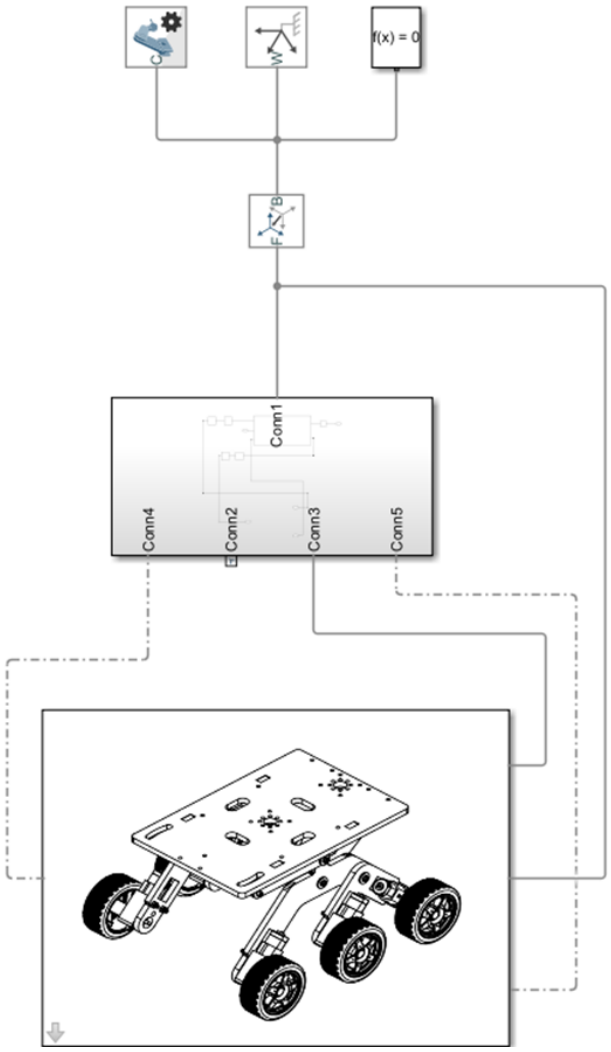

Figure 3 – Multibody model scheme.

Fig. 3 shows the first level of modeling in Simulink, which consists of three macroblocks:

- World Frame, System Config. and Solver;
- Environment Multibody;
- Rover Multibody.

In the second macroblock, the ground and obstacles were modeled.
The third macroblock is composed of the multibody models of the chassis, the six wheels with their own wheel-to-ground contact. Moreover, there are the six Simscape® DC-motors and gearboxes models.

3 Experimental Phase

The embedded LSM6DS3TR IMU on Arduino board was used as sensor to compare the obtained experimental results and simulations output. Through the IMU, It is possible to acquire translational accelerations and rotational velocities along and around the three fundamental axes. The reference system used, and shown in Fig. 4, is the same as that shown on the Arduino board.

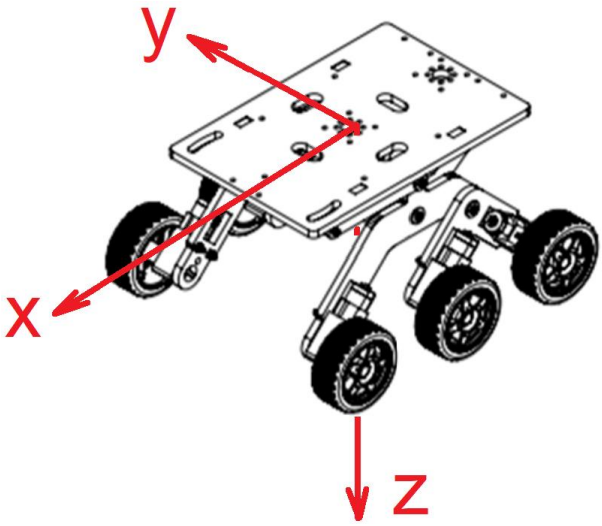

Figure 4 – IMU sensor reference frame.

The obtained accelerometer signals from the prototype and the model, were acquired in front-rocker and front-bogie configurations in a straight-line motion. Table 1 summarizes the acquired signals.

Table 1 – Signal acquisition parameters

SIGNAL	FRONT CONFIGURATION	SOURCE	SAMPLING FREQUENCY [Hz]	SUPPLY VOLTAGE [V]	NO-LOAD SPEED [RPM]
1	Bogie	Model	90	6	230
2	Rocker	Model	90	6	230
3	Bogie	Prototype	400	6	230
4	Rocker	Prototype	400	6	230

The no-load speed used in the last column of the Table 1 are available in the data sheet of the DC electric motor. Signals three and four were sampled by the IMU and the FFT was performed on the Arduino board in Real-Time and then saved on an SD card connected to the controller.

4 Results

The sampled accelerometer signals were analyzed by the Fast Fourier Transform (FFT) with the aim of showing the presence of isolated peaks in the Transform, which were found to be the rotational frequencies of the wheels. The analysis of the accelerometer signals was carried out for all three directions in space, but only y-axis will be shown below because more significant. Fig. 5 shows the FFT of signals 1 and 2 from Table 1. In both FFTs, despite the low sampling rate and the presence of noise, two peaks corresponding to a frequency of 3.7 Hz are clear in both configurations. In the Fig. 5 (left) the rover advances with the bogie at the front; in the Fig. 5 (right) it advances with the rocker at the front.

$$RPS_{nom} = \frac{RPM_{nom}}{60} = \frac{230}{60} = 3.8\, rps = 3.8\, Hz$$

$$\%E = \frac{|RPS_r - RPS_{nom}|}{RPS_{nom}} \cdot 100 =$$

$$= \frac{|3.7 - 3.8|}{3.8} \cdot 100 = 2.6\,\%$$

The $RPS_{nom}$is obtained by no-load speed at 6 DC Voltage as in the electric motor datasheet. The RPS_r corresponds to the real peak frequency obtained by FFT analysis. The difference between the theoretical value obtained from the motor data sheet and that of the simulation is only 0.1 Hz, that leads to a percentage error of 2.6 %. The achieved result provides insight to validate the multibody model.

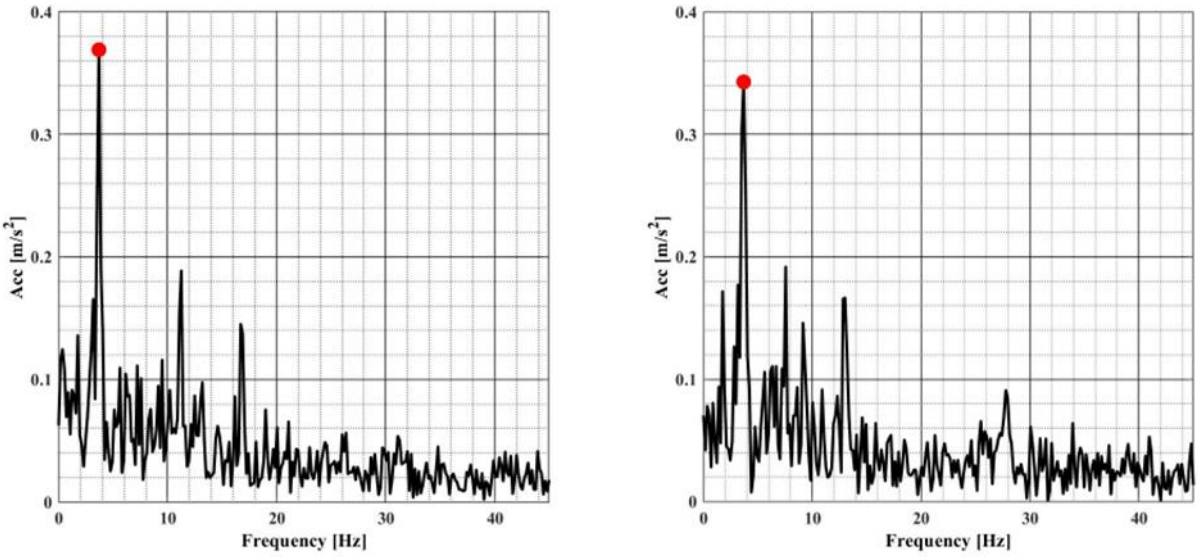

Figure 5 – FFTs calculated on accelerometer signals of model in straight line motion: left) bogie front; right) rocker front.

In Fig. 6 is shown the FFT of signals 3 and 4 from Table 1. The two peaks are clearly recognizable, respectively at 87.8 Hz ($f_{PEAK}(BF)$) for bogie at the front Fig. 6 (left) and 83.1 Hz ($f_{PEAK}(RF)$) for rocker at the front Fig. 6 (right).

These two values are significantly higher than the previously nominal values of 3.8 Hz. This discrepancy can be addressed to the fact that on the generic rover wheel tire tread there are four lines of twenty-four tire blocks circumferentially organized (Fig. 7).

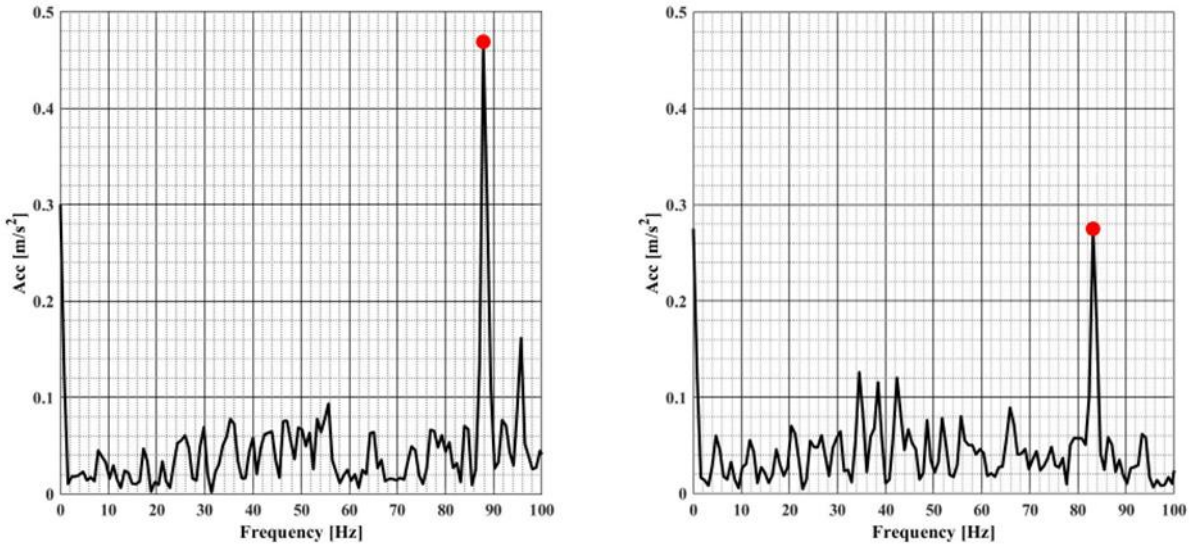

Figure 6 – FFTs calculated on accelerometer signals of prototype in straight line motion: left) bogie at the front; right) rocker at the front.

It can be said that the sensor (IMU), during only one wheel rotation, can detect the contact between the individual block and the ground, an event that is repeated 24 times in one revolution of the tire.
Indeed, in case of bogie at the front:

$$f = \frac{f_{PEAK}(BF)}{N_{blocks}} = \frac{87.8}{24} = 3.6\ Hz$$

In case of rocker at the front:

$$f = \frac{f_{PEAK}(RF)}{N_{blocks}} = \frac{83.1}{24} = 3.5\ Hz$$

Figure 7 – Rover wheel tire tread with four lines of twenty-four tire blocks circumferentially organized.

The differences between the real and nominal values, 0.2 Hz in the first case and 0.3 Hz in the second, could be due to the backlash between the Rocker-Bogie suspension components, the deformability of the parts (in the model they were assumed rigid), and the non-uniform distribution of grease within the gearbox in each of the six motor groups.

$$\%E_{BF} = \frac{|RPS_r - RPS_{nom}|}{RPS_{nom}} \cdot 100 = \frac{|3.6 - 3.8|}{3.8} \cdot 100 = 5.2\ \%$$

$$\%E_{RF} = \frac{|RPS_r - RPS_{nom}|}{RPS_{nom}} \cdot 100 = \frac{|3.5 - 3.8|}{3.8} \cdot 100 = 7.8\ \%$$

The percentage errors in the experimental tests are higher than the simulation case. The reason of such difference could be addressed to a lower modelled friction than the actual friction in the experimental setup.
This analysis is still valid in the case of the rover performs a skid steering where the two sides are at different speeds. For this purpose, it was decided to acquire from the embedded IMU, by frequency of 90 Hz, a signal, post-processed by FFT in MatLab®, during a left-hand steering in a configuration with bogie at the front.
In this case, the motors on the right side were supplied by 2.6 V, that corresponds to 93 rpm, and

those on the left by 1.6 V, that are equal to 57 rpm. Such wheel speeds correspond to a frequency of 1.5 Hz and 0.95 Hz, respectively. Once the accelerometer signal acquisition process was completed, the FFT shown in Fig. 8 was computed.

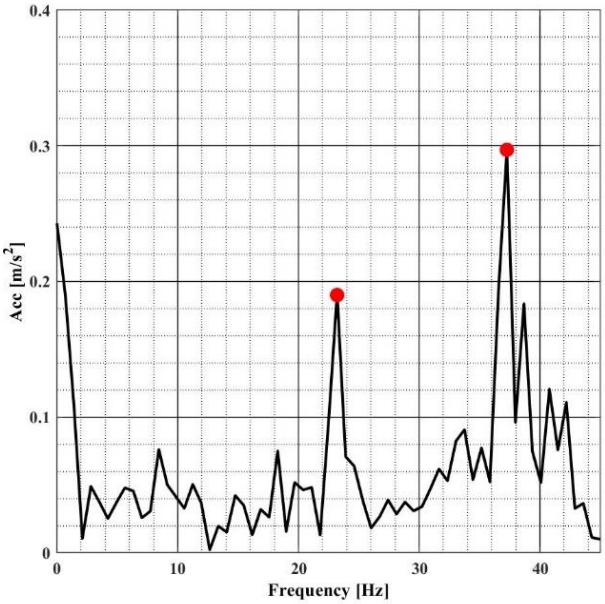

Figure 8 – FFT calculated on accelerometer signal of prototype in skid steering maneuver with bogie at the front.

In Fig.8, two peaks are clearly distinguishable: the first peak corresponds to 23.2 Hz, while the second one corresponds to 37.3 Hz. Such test is still characterized by the presence of the multiplicative factor due to the number of the tire tread blocks. Thus, dividing these values by 24, the real frequency values are 0.96 and 1.55 Hz. Both differs by only 0.01 Hz from expected values, which the first is 0.95 Hz, while the second is 1.54 Hz; that leads to percentage error calculation for both Left and Right sides.

$$\%E_L = \frac{|RPS_r - RPS_{nom}|}{RPS_{nom}} \cdot 100 = \\ = \frac{|0.96 - 0.95|}{0.95} \cdot 100 = 1\ \%$$

$$\%E_R = \frac{|RPS_r - RPS_{nom}|}{RPS_{nom}} \cdot 100 = \\ = \frac{|1.55 - 1.54|}{1.54} \cdot 100 = 0.6\ \%$$

5 Conclusions

This work dealt with the study of the motion sensing of a mobile robot through simulation and experimental combined approach.

The analysis on the accelerometer signals made it possible to show, both experimentally and in simulation, that by means of FFT analysis, it was possible to distinguish sharply peaks in the Transform. These frequencies corresponded to the rover wheel rotations. In simulation, these frequencies were completely coincident with those obtained theoretically from the data sheet of the electric DC motors, while in the experimental tests they were multiplied by 24, which is the number of the tire tread blocks.

These results were still valid both in the case of bogie and rocker at the front. In addition, during the skid steering test, it was possible to distinguish two peaks in the FFT whose frequencies corresponded to the two different rotational speeds of the wheels on the two sides.

The computed parameters through the proposed Real-Time signal processing approach could aid the motion planning and rover navigation control in a future perspective.

References:

[1] Liu, Y.; Ma, X.; Shu, L.; Hancke, G.P.; Abu-Mahfouz, A.M. From Industry 4.0 to Agriculture 4.0: Current Status, Enabling Technologies, and Research Challenges. IEEE Trans. Ind. Informatics 2021, 17, 4322–4334, doi:10.1109/TII.2020.3003910.

[2] Navas, E.; Fernández, R.; Sepúlveda, D.; Armada, M.; Gonzalez-de-Santos, P. Soft Grippers for Automatic Crop Harvesting, A Review; Sensors 2021, 21, 2689.

[3] Friha, O.; Ferrag, M.A.; Shu, L.; Maglaras, L.; Wang, X. Internet of Things for the Future of Smart Agriculture: A Comprehensive Survey of Emerging Technologies. IEEE/CAA J. Autom. Sin. 2021, 8, 718–752.

[4] Califano F, Cosenza C, Niola V, Savino S. Multibody Model for the Design of a Rover for Agricultural Applications: A Preliminary Study. Machines. 2022; 10(4):235. https://doi.org/10.3390/machines10040235

[5] Bechar, A.; Vigneault, C. Agricultural robots for field operations: Concepts and components. Biosyst. Eng. 2016, 149, 94–111.

[6] Kan, X.; Thayer, T.C.; Carpin, S.; Karydis, K. Task Planning on Stochastic Aisle Graphs for Precision Agriculture. IEEE Robot. Autom. Lett. 2021, 6, 3287–3294.

[7] Bac, C.W.; Hemming, J.; van Tuijl, B.A.J.; Barth, R.; Wais, E.; van Henten, E.J. Performance Evaluation of a Harvesting Robot for Sweet Pepper. J. F. Robot. 2017, 34, 1123–1139, doi:10.1002/rob.21709.

[8] SILES, IVAN, and IAND WALKER, "Continuum Robotic Elements for Enabling Negotiation of Uneven Terrain in Unstructured Environments." Issue

4, Volume 8, October 2013, E-ISSN: 2224-3429, WSEAS TRANSACTIONS on APPLIED and THEORETICAL MECHANICS

[9] Toupet, Olivier. "An Overview of the Mars 2020 Perseverance Rover's Enhanced Path-Planner." (2020).

[10] Jacobstein, Neil. "NASA's Perseverance: Robot laboratory on Mars." *Science* Robotics 6.52 (2021): eabh3167.

[11] Bickler, D.B. Articulated Suspension System, Patent: 4840394, USA 1989, 1–6.

[12] Bruzzone, Luca, and Giuseppe Quaglia. "Locomotion systems for ground mobile robots in unstructured environments." Mechanical sciences 3.2 (2012): 49-62

[13] D. S. Chinchkar, S. S. Gajghate, R. N. Panchal, R. M. Shetenawar, P. S. Mulik, Design of Rocker Bogie Mechanism, International Advanced Research Journal in Science, Engineering and Technology, National Conference on Design, Manufacturing, Energy & Thermal Engineering (NCDMETE-2017), Vol. 4, Special Issue 1, 2017, pp. 46-50.

[14] N. Yadav , B. Bhardwaj, S. Bhardwaj, Design analysis of Rocker Bogie Suspension System and Access the possibility to implement in Front Loading Vehicles, IOSR Journal of Mechanical and Civil Engineering (IOSR-JMCE), Vol. 12, N. 3, 2015, pp. 64-67.

[15] K. Harish Chandu, P. Hari Narayana, K. C. Charan Teja, B. Sai, Y. Murali Mohan, Design and Fabrication of Rocker Bogie Mechanism, International Journal of Scientific Engineering and Technology Research, Vol. 7, N. 4, 2018, pp. 781-84.

[16] Cosenza C, Nicolella A, Esposito D, Niola V, Savino S. Mechanical System Control by RGB-D Device. Machines. 2021; 9(1):3. https://doi.org/10.3390/machines9010003

[17] Cumani, Aldo, and Antonio Guiducci. "Fast stereo-based visual odometry for rover navigation." WSEAS Trans Circuits Syst 7.7 (2008): 648-657.

[18] C. Chen, M. Shu, Y. Wang, L. Ding, H. Gao, H. Liu, S. Zhou, Simultaneous control of trajectory tracking and coordinated allocation of rocker-bogie planetary rovers, Mechanical Systems and Signal Processing, Vol. 151, 2021

[19] S. Wu, L. Li, Y. Zhao, M. Li, Slip ratio based traction coordinating control of wheeled lunar rover with rocker bogie, Advanced in Control Engineeringand Information Science, Vol. 15, 2011, pp. 510-15.

[20] Cosenza, Chiara, Vincenzo Niola, and Sergio Savino. "Modelling friction phenomena in an underactuated tendon driven finger by means of vision system device data." The International Conference of IFToMM ITALY. Springer, Cham, 2018.

[21] Cosenza, Chiara, Vincenzo Niola, and Sergio Savino. "Underactuated finger behavior correlation between vision system based experimental tests and multibody simulations." IFToMM Symposium on Mechanism Design for Robotics. Springer, Cham, 2018.

[22] Niola V., Rossi C., Savino S., Troncone S., An underactuated mechanical hand: A first prototype, 23rd International Conference on Robotics in Alpe-Adria-Danube Region, 2014.

[23] M. Thianwiboon, V. Sangveraphunsir, Traction Control of a Rocker-Bogie Field Mobile Robot, Thammasat Int. J. Sc. Tech., Vol. 10, No. 4, 2005, pp. 48-59.

[24] A. Nicolella, V. Niola, S. Pagano, S. Savino, M.Spirito An overview on the kinematic analysis of the rocker-bogie suspension for six wheeled rovers approaching an obstacle. Advances in Italian Mechanism Science in Proceedings of the 4th International Conference of IFToMM Italy Mechanisms and Machine Science vol. 122

[25] C. Cosenza, V. Niola, S. Pagano, S. Savino. Spring-loaded rocker-bogie suspension for six wheeled rovers. Advances in Italian Mechanism Science in Proceedings of the 4th International Conference of IFToMM Italy Mechanisms and Machine Science vol. 122

[26] Amoresano, A., Niola, V., Quaremba, A. (2012). A sensitive methodology for the EGR optimization: A perspective study. *International Review of Mechanical Engineering*, *6*(5), 1082-1088.

[27] O.Elshazly et al. "Skid steering mobile robot modeling and control" UKACC International Conference on Control. Loughborough, U. – 2014

Contribution of Individual Authors to the Creation of a Scientific Article (Ghostwriting Policy)

The author(s) contributed in the present research, at all stages from the formulation of the problem to the final findings and solution.

Sources of Funding for Research Presented in a Scientific Article or Scientific Article Itself

No funding was received for conducting this study.

Conflict of Interest

The author(s) declare no potential conflicts of interest concerning the research, authorship, or publication of this article.